

## Compact Laser Radar for Remote Atmospheric Probing

G. W. GRAMS AND C. M. WYMAN

National Center for Atmospheric Research,<sup>1</sup> Boulder, Colo. 80302

(Manuscript received 2 June 1972)

### ABSTRACT

A compact laser-radar system has been developed for use on an airborne platform. Of particular interest is the use of a flashlamp-pumped dye laser as the radiation source and a plastic Fresnel lens in the receiver to collect the radiation backscattered by the atmosphere. These novel features resulted in a laser probing system that is less expensive, more reliable, and more compact than systems incorporating ruby lasers and more conventional receiver optics.

### 1. Introduction

The laser is germane to a novel type of instrument that has evolved from exploratory efforts to develop techniques for probing the atmosphere by analyses of the light scattered from the beam by the various constituents of the atmosphere. Since the basic principle of operation of this type of atmospheric probe closely parallels that of a microwave radar, it is usually called a *laser radar* or *optical radar* (*lidar*, an acronym for *light detection and ranging* has also been used to identify this type of device). To conform with the most common usage, we refer to the device as a laser radar.

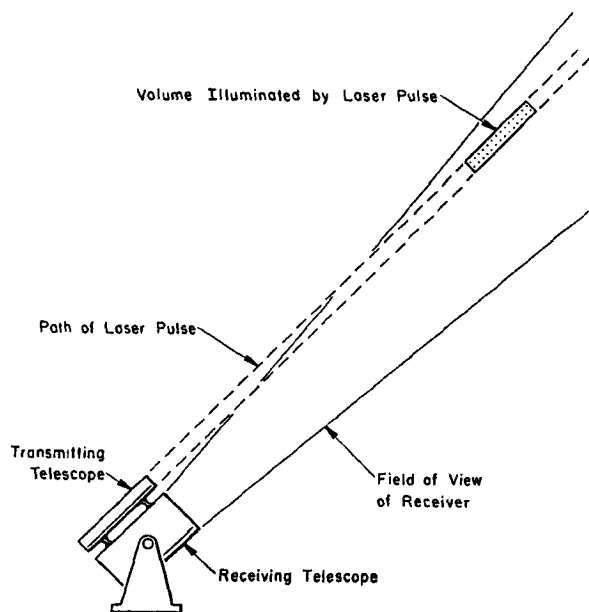


FIG. 1. Schematic illustration of a monostatic laser radar.

<sup>1</sup>The National Center for Atmospheric Research is sponsored by the National Science Foundation.

### 2. Principle of operation of a monostatic laser radar

In its simplest and most common form, the laser radar is aligned in a monostatic configuration whereby the optical axes of the transmitter and receiver are parallel. A typical monostatic laser-radar configuration is shown schematically in Fig. 1. The laser generates a short, highly collimated light pulse that propagates through the atmosphere and, at any instant, illuminates a well-defined volume containing both molecules and suspended materials (usually referred to as aerosols) such as liquid droplets and dust particles. The molecules and aerosols will backscatter a small amount of the laser radiation, which can be collected by a suitable receiving telescope. A typical receiver configuration is shown schematically in Fig. 2. The elements of the optical system in this schematic example are a primary lens  $l_1$  of radius  $r_1$  and focal length  $f_1$  to collect the backscattered radiation and a secondary lens  $l_2$  of radius  $r_2$  and focal length  $f_2$  located a distance  $f_1 + f_2$  behind  $l_1$  to collimate light collected from volume at large distances, relative to  $f_1$ , from the telescope. This light is then passed through a narrow-band interference filter  $F$  to decrease the intensity of background light from the sky. Laser-radar receivers are normally afocal telescopes since the transmission of narrow-band interference

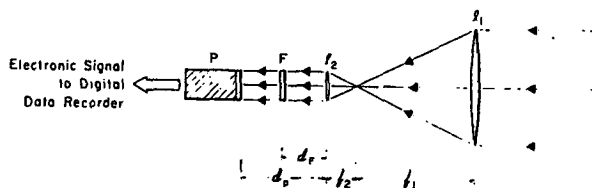


FIG. 2. Schematic illustration of typical receiver configuration. The primary lens  $l_1$  of focal length  $f_1$  collects light backscattered by atmospheric constituents. The secondary lens  $l_2$  of focal length  $f_2$  recollimates the light focused by  $l_1$ . The collimated light is directed through a narrow band interference filter  $F$  and then onto the face of a photomultiplier  $P$ .

filters varies as a function of the angle of incidence and collimated light at the filter is thereby necessary. After passing through the interference filter, the transmitted light is directed onto the face of a photomultiplier tube P, and the intensity of the light at the laser wavelength is thereby measured. The signal from the photomultiplier can be amplified and displayed as a function of time on an oscilloscope; the range associated with the instantaneous intensity of the laser echoes can be determined by measuring the time interval from laser pulsing. Permanent records of the laser echoes can be obtained by photographing the oscilloscope display; some of the more sophisticated laser-radar systems that have recently been developed incorporate on-line digital electronic computers or record digitized laser echoes on magnetic tape for subsequent computer processing.

The analysis of data obtained with these active probing systems is quite straightforward. The laser radar provides a measurement of the optical backscattering cross section of the atmospheric constituents as a function of altitude. The intensity of the echoes of an optically thin layer of homogeneously distributed scatterers, expressed in terms of the expected rate of emission of photoelectrons per transmitted laser pulse, is

$$\frac{dn_p}{dt} = \frac{WK_1K_2A\eta\lambda}{8\pi h} \cdot \frac{K_a^2\Sigma}{R^2}, \quad (1)$$

where  $W$  is the transmitted energy per pulse,  $K_1$  and  $K_2$  the efficiencies of the receiving and transmitting systems,  $A$  the collecting area of the receiving telescope,  $\eta$  the quantum efficiency of the photocathode,  $\lambda$  the wavelength,  $K_a$  the integrated atmospheric transmission between the transmitter and the sample volume located at range  $R$ ,  $\Sigma$  the collective radar cross section of the scatterers per unit volume, and  $h$  Planck's constant. The above "radar equation" has been derived elsewhere (Grams, 1966); only  $K_a$ ,  $\Sigma$  and  $R$  are range-dependent.

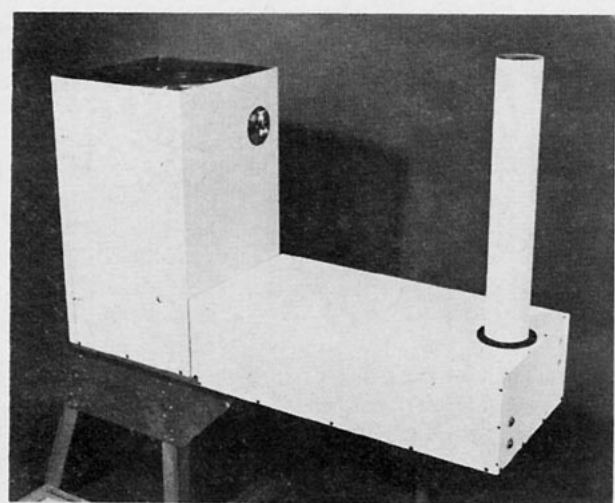


FIG. 3. Photograph of the NCAR compact laser radar transmit-receive unit.

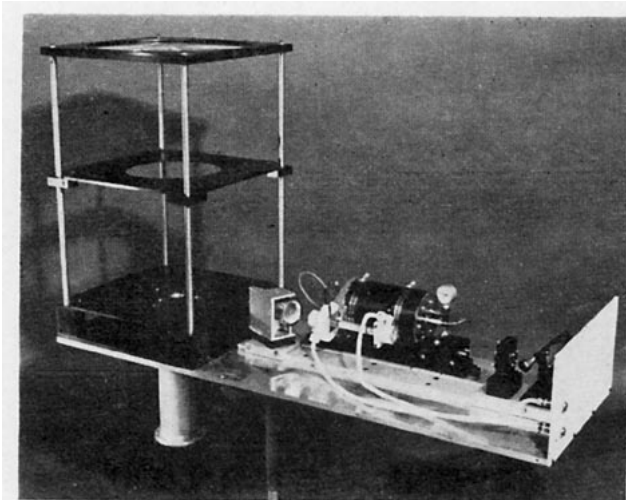


FIG. 4. Photograph of transmit-receive unit with covers removed to show the basic elements of the system.

The value of  $\Sigma$  is determined by the contributions to backscattering from the various atmospheric constituents. For a dust-free atmosphere, we would have

$$\Sigma = N\sigma_R,$$

where  $N$  is the molecular number density and  $\sigma_R$  the radar cross section of an individual air molecule evaluated in accordance with Rayleigh scattering theory. Thus, the measured intensity would exhibit a smooth monotonic decrease with altitude and would provide data on the atmospheric density at each altitude. The vertical density profile could then be used to obtain vertical profiles of atmospheric temperature with the same technique used by Elterman (1953) to interpret data obtained by measurement and analyses of light scattered from searchlight beams. However, the interpretation of these echoes becomes more difficult when atmospheric aerosols are present. These materials can cause significant deviations from the echoes received from the molecular atmosphere and can therefore be detected by the apparatus. Thus, laser radars have often been used for studies of the temporal and spatial variability of aerosol layers in the upper atmosphere (Grams, 1970).

Observations of the optical backscattering by the atmosphere do not provide absolute measurements of the atmospheric aerosol content or of the density of the molecular atmosphere unless the effects of scattering by aerosols and atmospheric molecules can be separated. In general, the problem of separating the contributions of the molecular scatterers from those of the larger particles can be solved by taking advantage of their different scattering characteristics. In particular, measurements of the optical backscattering cross sections at two or more wavelengths, with reasonable assumptions about the physical characteristics of the atmospheric aerosols, can provide a means of establishing

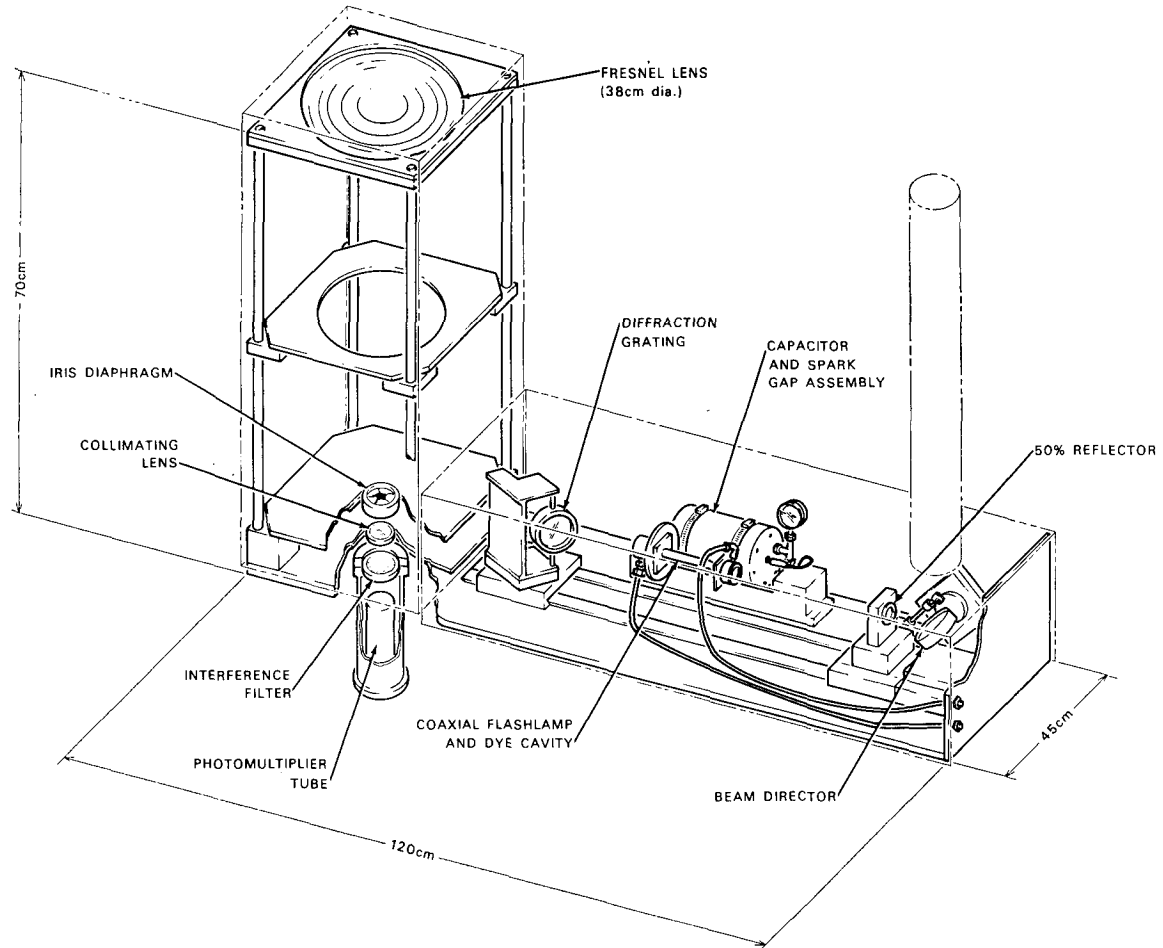


Fig. 5. Schematic drawing showing the major elements of the transmit-receiver unit. Approximate dimensions of the unit are shown; the unit weighs about 60 kg.

the relative contributions of molecular and aerosol scattering. If the separation can be effected, the density profiles so obtained may be used for deriving data on, for example, atmospheric temperature and pressure profiles. Recent developments in the field of tunable organic dye lasers opens the possibility of selecting the wavelength of the radiation emitted by the laser to effect such separations. We have developed a compact laser radar incorporating a pulsed dye laser, and we will present a description of some novel features of the system.

### 3. Description of the compact laser system

Fig. 3 shows a photograph of the transmit-receive unit of the laser radar. The receiver is on the left, and the laser beam is transmitted through the vertical pipe on the right. Fig. 4 is a photograph of the system with covers removed, and Fig. 5 a schematic drawing of the system. Approximate dimensions of the system are shown in Fig. 5; the entire transmit-receive unit weighs about 60 kg. The ancillary equipment necessary to operate this unit includes a Hipotronics R30B 100 W

laser power supply, a closed-loop dye circulating system, a photomultiplier power supply, a signal amplifier, a data acquisition system, and an electronic control panel. All this equipment can be mounted in one standard-size electronics rack.

The primary lens of the receiving telescope is seen in the upper left corner of Figs. 4 and 5. This lens is a Fresnel lens, which is basically a flat, thin piece of plastic on which has been molded a series of concentric stepped zones extending from the center to the edge. Fig. 6 illustrates the geometric relationship between the concentric zones on the Fresnel lens and the surface of an ordinary lens. Each zone refracts the incident light so that the combined action of each refracting facet will focus the light in essentially the same manner as a conventional lens. Lenses of this type have been widely used, for example, in overhead projectors and in rear-view projection screens and camera viewing systems for brighter, more uniformly illuminated images. However, the quality of this receiving telescope lens (manufactured by Fresnel Optics, Inc) was considerably better than that of lenses fabricated for the above-named

applications. Its focal length was about 61 cm, diameter 38 cm, and thickness about 1 cm. The lens, with concentric zones spaced at approximately  $2 \text{ lines mm}^{-1}$ , was capable of forming a sharp image for objects near the optical axis. Normally, a laser-radar receiver does not require a wide field of view for its required function of collecting the light scattered from the sample volume and directing it onto the face of the photomultiplier which, in our system, has an active area about 3 cm in diameter. The circle of least confusion for collimated light directed parallel to the optical axis has been measured to be only about 1 mm in diameter for monochromatic light of wavelength  $0.6328 \mu\text{m}$ . In the plane containing the circle of least confusion, the spatial distribution of the collected light is a bright spot of the above diameter with the surrounding area weakly illuminated by, presumably, light scattered at the edges of the concentric zones of the Fresnel lens. However, the flux density of this scattered light has been measured to be almost three orders of magnitude less than within the circle of least confusion. The imaging ability of the lens for off-axis radiation has not been fully evaluated, but our qualitative observations indicate noticeable degradation when the incident radiation makes an appreciable angle with the optical axis of the lens. Since laser-radar receivers do not require a wide field of view, this is not a serious problem for our application. Therefore, we feel that, although the Fresnel lens used in this system cost only about \$60.00, its quality is quite acceptable for use in laser-radar receivers.

The actual configuration of the dye laser used in the NCAR transmit-receive unit was based primarily on results of the developmental work on flashlamp-pumped organic dye lasers by Furumoto and Cecon (1969). The laser, shown photographically in Fig. 4 and schematically in Fig. 5, incorporates a Candela Corporation CL-100 xenon-filled coaxial flashlamp. The flashlamp is attached to a modified Candela Corporation ED-100 electric driver, which incorporates a 100-joule, 25-kV capacitor with a pressurized spark-gap switch.

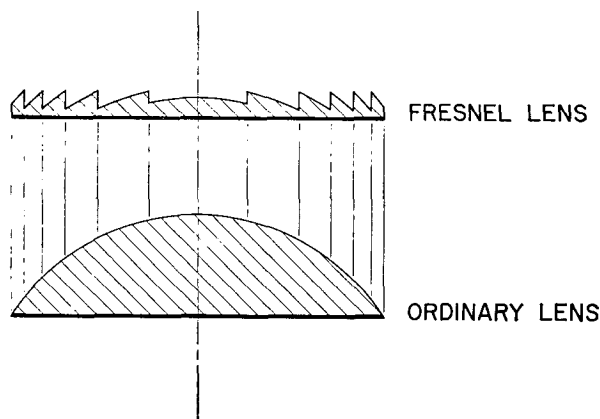


FIG. 6. Schematic drawing of a Fresnel lens. Concentric stepped zones form refracting facets which focus incident light in essentially the same manner as an ordinary lens.

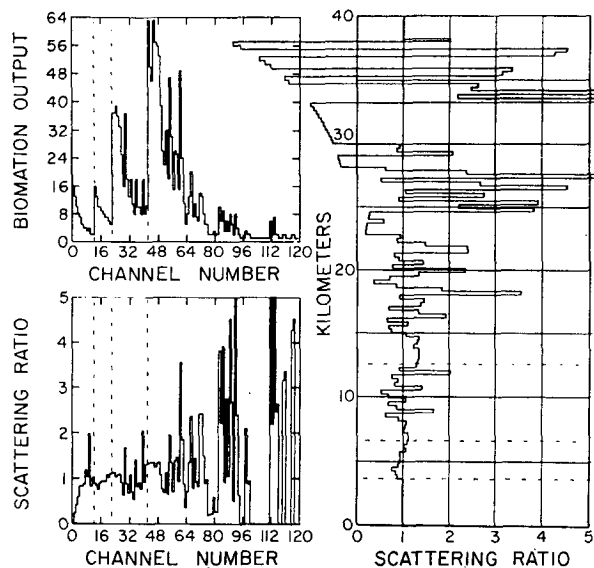


FIG. 7. Example of data obtained with compact laser-radar system from a single laser pulse.

The laser cavity consists of a diffraction grating, shown to the left of the flashlamp in Figs. 4 and 5, for one end mirror and a partially reflecting mirror, shown on the right in Figs. 4 and 5, for the output-coupling element. The diffraction grating is a PTR Optics Corporation TF-17 aluminum-coated grating with a groove spacing of  $1200 \text{ mm}^{-1}$ , a blaze angle of  $17\frac{1}{2}^\circ$ , and blaze wavelength of  $5000 \text{ \AA}$ . In the dye laser cavity, the diffraction grating acts as an end reflector for a narrow spectral region around a wavelength that varies with the grating angle of incidence. The laser can be tuned by rotating the diffraction grating about an axis parallel to the grooves. For this system, the spectral condensation produced by using the grating reduced the output linewidth to about  $1 \text{ \AA}$ .

The laser was operated at about  $5850 \text{ \AA}$  using Rhodamine 6G dye. The interference filter used in the receiver has a linewidth of about  $10 \text{ \AA}$  full-width-at-half-maximum and is centered at about  $5850 \text{ \AA}$ . Final laser tuning was accomplished by adjusting the angle of incidence on the grating to maximize the atmospheric echoes collected by the receiver and transmitted through the interference filter. The output wavelength stability was such that the fluctuations of laser echoes measured by the photomultiplier through the  $10 \text{ \AA}$  filter could be related only to the small (10% or less) shot-to-shot fluctuations in the laser output.

#### 4. Discussion

The laser radar was specifically designed for installation on the Convair 990 research aircraft operated by the National Aeronautics and Space Administration and has been used in a program of cooperative research by the University of Wisconsin and NCAR to provide

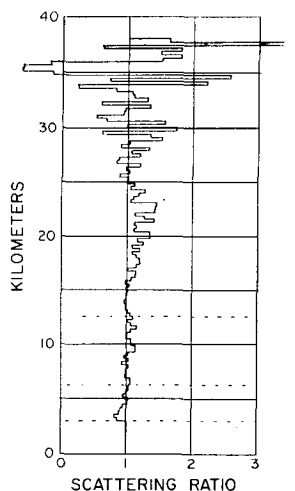


FIG. 8. Example of data obtained with compact laser-radar system from the average of 50 consecutive laser pulses during a 10-min interval.

data on the spatial distribution of the stratospheric aerosol layer. Preliminary results of that experiment have been presented by Fox *et al.* (1972). For these measurements, laser echoes were digitized with the University of Wisconsin Data Acquisition System (Fox and Eloranta, 1972), which incorporates a Biomation Model 610 transient recorder. Fig. 7 is an example of the type of data obtained for each laser pulse. The graph on the upper left shows the digitized echoes as a function of time after laser pulsing (or channel number) for pulse number 191 on day 223 (11 August 1971). The signal from an EMI 9658 photomultiplier was passed through a gain-switching amplifier before being digitized. The times at which the amplifier was switched to a higher gain to record the rapidly decreasing signal are indicated by the vertical dashed lines. For the example shown, each channel corresponds to 2- $\mu$ sec intervals although some data were also obtained at 1- $\mu$ sec intervals for higher range resolution. The data plotted in the graph on the lower left of Fig. 7 show the ratio of the gain-corrected signal to the signal expected from a dust-free atmosphere (a scattering ratio of 1 implies molecular scattering only) calculated in accordance with Eq. (1). The same information is plotted on the right of Fig. 7 with channel numbers converted to the altitude from which the echo was received. Data obtained in the first gain-switch interval have not been plotted as the laser beam was not fully contained in the field of view of the receiver until about 2 or 3 km above the aircraft. If beam overlap at a shorter range is desired, the position of the elements along the optical axis or the laser cavity should be reversed from the locations illustrated in Figs. 4 and 5 so that the output beam director is located as close as possible to the laser receiver. It can be seen that the laser radar, in the configuration used in the Convair 990 flights, is able to "see" to a range of about 20 km above the aircraft before the signal falls to noise

levels. Fig. 8 shows data averaged over 50 consecutive pulses (a 10-min interval at the 0.2  $\text{sec}^{-1}$  pulse rate used in these flights) for the same date (pulse numbers 191–241, day 223). It is seen that the noisy character of the signal is improved by the averaging with a definite indication of enhanced scattering in the 20–25 km region, as had been expected for the latitude of Hawaii where the above data were obtained. The data used in the example were obtained at the surface before take-off on the indicated date. Approximately 14,000 laser echoes were digitized and recorded at 5-sec intervals with the laser radar system described above on four aircraft flights from Hawaii to about 9N and two other flights from Wallops Island, Va., to Bermuda at flight altitudes which varied from 10–13 km.

This compact laser radar has demonstrated the advantages of incorporating the recently developed flashlamp-pumped organic dye laser into atmospheric probing systems. The aspect of organic dye lasers that has received the most attention to date has been their ability to tune the output over a wide range of wavelengths. This ability has been exploited, for example, in measurements of the vertical structure of the layer of sodium atoms present in the atmosphere at about 90 km altitude by measuring its resonant interaction with the beam of a pulsed dye laser tuned to a sodium D-line. Laser-radar measurements now provide sodium profiles that are more accurate than those obtained by expensive, isolated rocket measurements or by photometric twilight studies of the sodium layer (Gibson and Sandford, 1971; Hake *et al.*, 1971).

In view of the excitement generated by the potential of the ability to tune the output wavelength of organic dye lasers, the other practical advantages of pulsed dye lasers have often been overlooked. Most laser-radar systems (with the most notable exception being those recently developed for the high-altitude sodium probes) use the ruby laser, which operates at a wavelength of 0.6943  $\mu\text{m}$ , as the radiation source. We therefore should discuss the advantages of the dye laser system relative to the capabilities of ruby laser systems. In the configuration shown in Figs. 4 and 5, the dye laser could generate 0.25 J pulses of duration somewhat less than 1  $\mu\text{sec}$  at a maximum pulse repetition rate of about 1  $\text{sec}^{-1}$  at 5850  $\text{\AA}$  using a  $5 \times 10^{-5} M$  solution of Rhodamine 6G dye in methanol. Even though much shorter pulse durations are possible with ruby lasers, a duration of 1  $\mu\text{sec}$  implies a range resolution of 150 m—a resolution compatible with practical limitations imposed by all but a few of the most advanced and expensive data acquisition systems in current use for recording laser-radar echoes.

As an example, the ruby system used by Fiocco and Grams (1969) generated 2 J pulses at 6943  $\text{\AA}$  of less than 100-nsec duration and at a maximum pulse repetition rate of about 0.5  $\text{sec}^{-1}$ . The power required to operate that system was measured in kilowatts, whereas the capacitor in the dye laser's electric driver was

charged with a 100 W power supply. Yet the average power radiated by the dye laser is only a factor of 4 less than that of the ruby system used in the example. To compensate for this factor, the photomultiplier quantum efficiency is less than 3% at the ruby wavelength of 6943 Å and increases rapidly with decreasing wavelength to more than 7% at 5850 Å for the S-20 photocathodes that have normally been used in laser-radar receivers. Thus, the increased detector sensitivity compensates somewhat for the lower average power, and the dye laser system requires at least an order of magnitude less power than systems using a ruby laser with approximately the same characteristic operating times  $\tau$ , as defined by Sandford (1967), to achieve a standard level of performance. In addition, the ruby laser must be cooled by closed-loop circulation of distilled water to operate at the pulse repetition rate used for our example. This coolant must be maintained at a constant temperature through the use of a water cooler requiring kilowatts more of power. With only about 100 W of heat to dissipate, the dye laser in the NCAR compact system was able to operate without any cooling apparatus whatsoever. In addition, the physical dimensions and weight of the dye laser and its ancillary equipment are also at least an order of magnitude less than for the ruby system used for our comparison.

## 5. Conclusions

Dye lasers are appreciably less expensive and less complex than the ruby lasers commonly used in laser-radar systems. Complete flashlamp-pumped dye laser systems with power supplies and dye circulation systems capable of producing light pulses of over 1 J are now available commercially for about \$5000, substantially less than comparable ruby lasers. With the use of a dye laser for the pulsed light source and an inexpensive plastic Fresnel lens to collect the backscattered light, laser radars can now be built which are less expensive, more reliable, and more compact than was heretofore possible. Since the development of a laser radar normally represents a considerable investment of time and financial resources we feel that many features of the compact system described above will be of interest

to investigators who have previously not been able to afford such investments for experimental studies of the atmosphere.

*Acknowledgments.* The authors wish to thank H. W. Furumoto and H. L. Ceccon for their role in developing our dye laser system. We feel that the demonstrated reliability of the airborne laser radar was directly associated with a system design that evolved from frequent discussions with them on the operation of flashlamp-pumped dye lasers.

Our decision to use the Fresnel lens as the primary lens of the compact laser radar grew out of discussions with F. B. Pearson. Helpful discussions on the receiver optics with J. H. Rush and C. E. Sheldon are also gratefully acknowledged.

## REFERENCES

- Elterman, L., 1953: A series of stratospheric temperature profiles obtained with the searchlight technique. *J. Geophys. Res.*, **58**, 519-530.
- Fiocco, G., and G. Grams, 1969: Optical radar observations of mesospheric aerosols in Norway during the summer, 1966. *J. Geophys. Res.*, **74**, 2453-2458.
- Fox, R. J., and E. W. Eloranta, 1972: A lidar digital data acquisition system. Paper presented at the Fourth Conference on Laser Radar Studies of the Atmosphere, Tucson, Ariz.
- , G. W. Grams, B. G. Schuster and J. A. Weinman, 1972: Airborne measurements of the stratospheric aerosol. Paper presented at the Fourth Conference on Laser Radar Studies of the Atmosphere, Tucson, Ariz.
- Furumoto, H. W., and H. L. Ceccon, 1969: Optical pumps for organic dye lasers. *Appl. Optics*, **8**, 1613-1623.
- Gibson, A. J., and M. C. W. Sandford, 1971: The seasonal variation of the night-time sodium layer. *J. Atmos. Terr. Phys.*, **33**, 1675-1684.
- Grams, G. W., 1966: Optical radar studies of stratospheric aerosols. Ph.D. thesis, Dept. of Meteorology, Massachusetts Institute of Technology.
- , 1970: Laser radar studies of the atmosphere above 50 km. *J. Atmos. Terr. Phys.*, **32**, 729-736.
- Hake, R. D., Jr., E. K. Proctor and R. A. Long, 1971: Tunable dye lidar techniques for measurement of atmospheric constituents. Paper presented at the Society of Photooptical Instrumentation Engineer's Seminar-in-Depth on Remote Sensing of Earth Resources and the Environment, Palo Alto, Calif.
- Sandford, M. C. W., 1967: Optical radar performance in atmospheric scattering. *J. Atmos. Terr. Phys.*, **29**, 1651-1656.